Supplemental Methods

Preparation and labelling of RT and nucleic-acid substrates. The H-labelled RT was derived from a mutant enzyme in which a single-residue modification E478Q[30] was introduced to the RNase H domain to inhibit the RNase H activity. This modification was employed to prevent substrate cleavage during the single-molecule measurement. To engineer the H-labelled RT, native cysteine residues located at positions 38 and 280 were changed to serine and a unique cysteine residue was introduced at the C-terminus of the p66 subunit to allow specific dye labelling through a thiol-maleimide reaction[39]. F-labelled RT was created from a similar mutant containing a unique cysteine at position 38 of the p66 subunit. Purified RT was incubated with Cy3-maleimide (GE Healthcare) and allowed to react for 60 minutes in a 100 mM phosphate buffer (pH 7). The Cy3-labeled RT was then purified by dialysis for more than 48 hours to remove the unreacted dye molecules. The p51 subunit was unlabeled.

Synthetic DNA (Qiagen Operon) and RNA (Dharmacon) oligonucleotides were purified by polyacrylamide gel electrophoresis (PAGE). All template strands (50 nt long) contained a biotin attached to the 3′ end as well as an internal amino modifier (dT C6). The amine group was labelled with a monoreactive Cy5 as per manufacturer's instructions (GE Healthcare) and the labelled template strands were HPLC purified by reverse phase chromatography on a C-8 column (GE Healthcare). The primer stands (19 – 21 nt long) were annealed to the template stands (in 10 mM TRIS pH 8, 80 mM NaCl, 1 mM EDTA) at a ~15:1 ratio at 60 °C for 10 minutes, cooled to < 30 °C over approximately 1 h, and stored in -20 °C. Removal of unannealed primer stands was not necessary as they did not contain either dye molecules or biotin groups for surface immobilization.

Single-molecule FRET measurements of RT-substrate binding orientation. Quartz slides were cleaned using argon plasma (Harrick Scientific), treated with 1% (w/v) Vectabond (Vector Laboratories) in acetone, rinsed, and incubated with a 20% (w/v) methoxy-PEG (M_r 5000;

Nektar Therapeutics) and 0.2% biotin-PEG (M_r 5000; Nektar Therapeutics) in 0.1 M sodium bicarbonate (pH 8.4) for at least 3 h. Streptavidin (0.2 mg/ml; Molecular Probes) and BSA (0.5 mg/mL, New England Biolabs) in 10 mM Tris (pH 8) and 10 mM NaCl was applied to the slide before immobilization of the biotinylated primer-template complexes (50 pM).

Donor and acceptor fluorescence signals were collected on a prism-type TIRF microscope. The FRET donor Cy3 was excited by a 532 nm YAG laser (Crystal Laser) and direct excitation of Cy5 was carried out by a 635 nm laser (Coherent). Emissions from donor and acceptor were separated using dichroic mirrors (Chroma Technology) and imaged onto the two halves of an Andor Ixon 887 back-illuminated electron multiplying CCD. The FRET value was defined as $I_A/(I_A + I_D)$, where I_A and I_D were the fluorescence signals detected from the acceptor and donor channel, respectively.

During image acquisition, Cy3-labelled RT (6 – 24 nM) was added to the sample containing surface-immobilized primer-template complexes in an imaging buffer containing 40 mM NaCl, 50 mM TRIS pH 8.0, 6 mM $MgCl_2$, 0.1 mg/mL BSA, 10% w/v glucose, ~1.5 mM Trolox (Sigma Aldrich)[40]. An oxygen scavenger system (300 µg/ml glucose oxidase, and 40 µg/ml catalase) was also added to the sample to reduce photobleaching. Positions of Cy5-labelled primer-template complexes were initially located using direct excitation of Cy5 with the 635 nm laser. FRET between Cy3 and Cy5 and fluorescence of Cy5 from direct excitation were then monitored by alternating the 532 nm and 635 nm excitations.

By increasing the intensity of the 532 nm excitation, photo-bleaching of Cy3 on the p66 subunit could be induced, shortening the duration of the observed fluorescence signal during a binding event. Under these conditions, Cy3 photobleaching was observed to occur in a single step as manifested by the one-step decrease of the fluorescence signal to the background level, indicating that only one Cy3 dye was present on the enzyme-substrate complex. We therefore conclude that the majority of the binding events involved one p66 subunit. Because the RT concentrations used in the single-molecule imaging experiments (10 – 20 nM) were far below

the equilibrium constant K_D for p66/p51 dimer formation (200 – 300 nM)[41], an excess of unlabeled p51 was added (~300 nM) to ensure that the majority of p66 subunits formed dimers with p51. Because the p66/p51 heterodimers are more stable than the p66/p66 homodimers, the probability of potential p66/p66 dimer formation during the experiment was thus minimal under these conditions. Finally, since the p66 and p51 subunits alone exhibited much lower affinities to the nucleic-acid substrates than the p66/p51 dimers, we thus conclude that the majority of the binding events observed in the experiments involve a single p66/p51 dimer.

DNA polymerase activity measurements by single-molecule FRET. To confirm that RT retains DNA polymerase activity on surface-immobilized primer-template complexes, we performed an in situ primer extension assay using single-molecule FRET. We designed a primer-template complex capable of reporting primer extension with FRET: The duplex region was labelled with Cy5, while Cy3 was placed on the 5′ end of the template, 10 nt away from the 3′ end of the primer, and 19 nt away from the Cy5 (Supplementary Fig. 2a). Extension of the primer by the DNA polymerase activity of RT converted the single-stranded region of the template to double-stranded, stretching the template and lowering the FRET from ~0.8 to ~0.5 (Supplementary Fig. 2b). To monitor primer extension in real time, FRET time traces from the primer-template complexes in a single field were recorded as 100 nM unlabeled RT and 250 μM dNTPs were added. The in situ primer extension rate was determined by averaging all trajectories that exhibited a strong fluorescent signal and non-zero FRET (to avoid complexes with bleached dyes) and fitting the average trace with a single-exponential decay. This rate was compared with the results obtained from the unimmobilized primer-template complexes incubated with unlabeled or Cy3-labelled RT using the gel electrophoresis assay, as described below (Supplementary Fig. 2c).

DNA polymerase activity measurements by gel electrophoresis. To measure the DNA polymerase activity of Cy3-labelled RT in comparison with unlabelled RT, 100 nM Cy3-labelled or unlabelled RT was preincubated in 150 μL imaging buffer (described above) containing 250

μM of each dNTP for 10 – 15 minutes. Extension of Cy5 end-labelled primer was initiated by the addition of 1.5 μL of 500 nM annealed primer-template complexes to the preincubated solution of RT and dNTP, and aliquots were removed at various time points, mixed in 90% vol/vol formamide, 1x TBE buffer and 10 mM EDTA to quench the reaction and heated to 90 °C for 1 min to denature the primer-template complexes. The products were then loaded on a pre-cast 10% polyacrylamide gel (8 M urea, Bio-Rad). Intensities of fluorescent bands were measured using a Typhoon gel scanner (GE Healthcare). This condition was used to provide a better comparison with the single-molecule in situ data where RT and dNTP were added to the surface-immobilized substrate simultaneously. We note that the apparent primer extension rates measured in these experiments reflects the convolution of the binding rate of RT to the substrate and the true rate of elongation by RT, and thus should be slower than the true elongation rate as probed in the following experiments.

To measure the DNA polymerase activity of the RT on substrates containing the 19D, 19R, 10R:9D or 9D:10R primers, 3 μM unlabeled RT was incubated in the imaging buffer with 500 nM primer-template complexes. The 5′ end of the primer strands were labelled with P^{32}. Primer extension was initiated by the addition of 1 mM dNTP. The reaction was quenched at various time points by the addition of 500 mM EDTA and formamide. The reaction products were heated to 90 °C for 1 min then separated on an 8% polyacrylamide gel. Radiolabeled primers were imaged on a phosphorimager cassette by a Typhoon gel scanner (GE Healthcare). The fraction of extended primers was quantified as a function of time. These data were fit to single-exponential decays with an offset to deduce the primer extension rate constant for each substrate. In the case of the 19R and 10R:9D primers, the fit was constrained to asymptote at a value of 0.8, which was the saturated fraction of extended primers for 19D and 9D:10R.

References:

39. Rausch, J. W., Sathyanarayana, B. K., Bona, M. K. & Le Grice, S. F. Probing contacts between the ribonuclease H domain of HIV-1 reverse transcriptase and nucleic acid by site-specific photocross-linking. *J. Biol. Chem.* **275**, 16015-16022 (2000).

40. Rasnik, I., McKinney, S. A. & Ha, T. Nonblinking and long-lasting single-molecule fluorescence imaging. *Nat. Meth.* **3**, 891-893 (2006).

41. Venezia, C. F., Howard, K. J., Ignatov, M. E., Holladay, L. A. & Barkley, M. D. Effects of efavirenz binding on the subunit equilibria of HIV-1 reverse transcriptase. *Biochemistry* **45**, 2779-2789 (2006)

Supplementary Information

Dynamic binding orientations determine the enzymatic activity of HIV reverse transcriptase

Elio A. Abbondanzieri, Greg Bokinsky, Jason W. Rausch, Jennifer X. Zhang, Stuart F. J. Le Grice, Xiaowei Zhuang

Supplementary Information Contents:

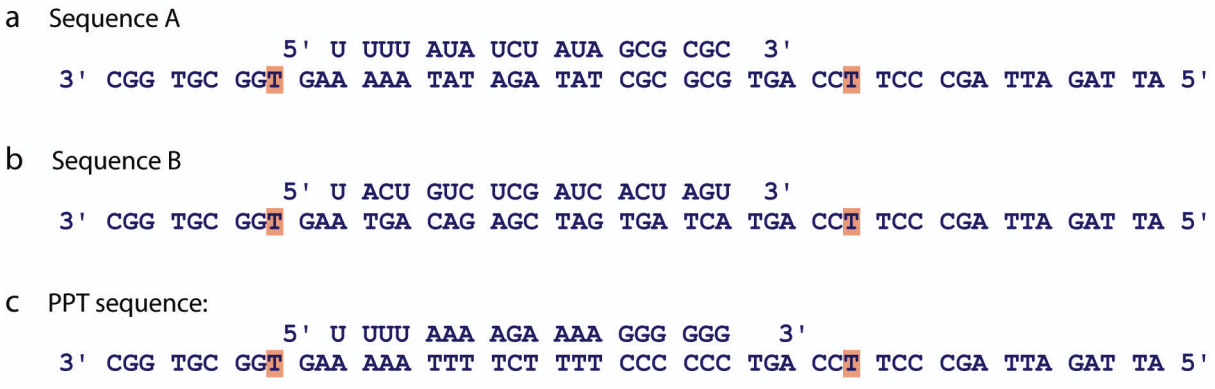

Supplementary Figure 1: Nucleic-acid substrate sequences used in experiments. Primer and template sequences were indicated in the upper and lower rows, respectively. The Cy5-attachement sites in the 5* and 3* labelling scheme are highlighted in red. Sequence A was used for experiments described in Fig. 2 and Supplementary Figs. 2-6. Sequence B was used for experiments described in Figs. 3 and 4 and Supplementary Figs. 6. The PPT sequence was used for experiments described in Fig. 5 and Supplementary Figs. 7-9.

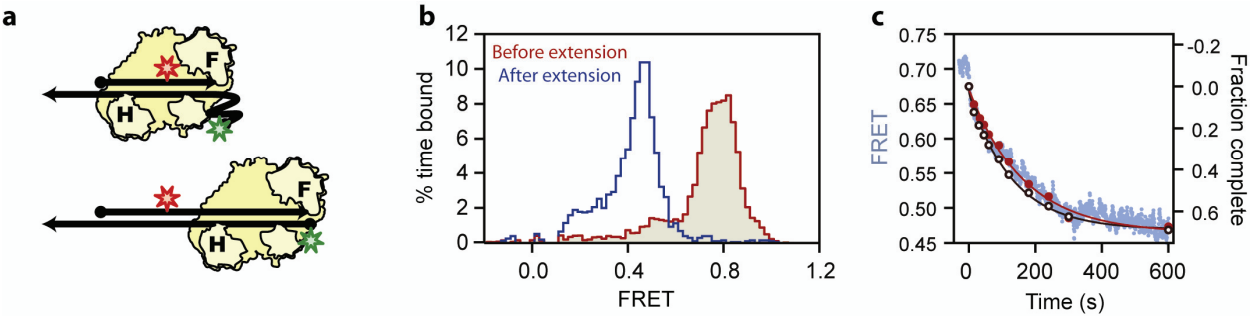

Supplementary Figure 2: Dye labelling and surface immobilization did not perturb the DNA polymerase activity of RT significantly. **a**, DNA-DNA primer-template complexes (black arrows) were labelled with both Cy3 (green star) and Cy5 (red star) and immobilized to a surface. Addition of RT and dNTP led to extension the DNA primer, and thus conversion of the ssDNA region to dsDNA, which shifted the two dyes further apart from each other, resulting in a decrease in FRET. **b**, FRET histograms of primer-template complexes before (red) and after (blue) the addition of unlabeled RT and dNTP. The main FRET peak shifted from ~0.8 to ~0.5 upon primer extension. **c**, The primer-extension kinetics measured from the *in situ* FRET assay are compared with those obtained from the gel electrophoresis assay. The light blue dots represent an average of 469 FRET traces from a single field of view. Unlabeled RT (100 nM) and 250 μM dNTP were added at 30 s. Fitting of the average FRET trace to a single-exponential decay gives an apparent primer-extension rate constant of 0.35 min^{-1}. Overlaid is the extension kinetics determined for unimmobilized primer-template complexes by gel electrophoresis using Cy3-labeled RT (red filled circles) or unlabeled RT (black unfilled circles). Fitting these two curves with single-exponential decay (red and black lines) gives extension rate constants of 0.34 min^{-1} and 0.46 min^{-1}, respectively. These results shows that the primer-extension kinetics obtained for unimmobilized and immobilized nucleic-acid substrates and for unlabelled and dye-labelled RT were all comparable, suggesting that the dye labelling and surface immobilization did not significantly perturb the DNA polymerase activity of RT. We note that the apparent primer extension rates measured in these experiments reflects the convolution of the binding rate of RT to the substrate and the true rate of elongation by RT. These rates are therefore slower than the elongation rate obtained when the reaction was initiated by addition of dNTP to the preincubated RT and substrate solutions, as shown in Fig. 4 in the main text.

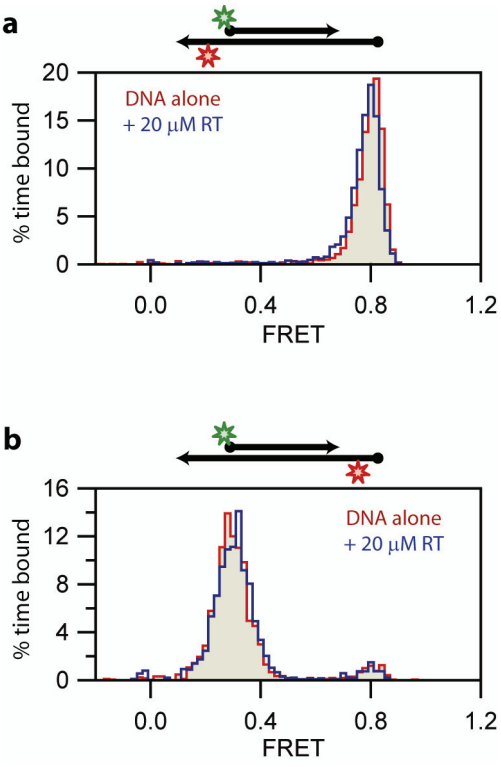

Supplementary Figure 3: Photo-physical properties of the FRET dyes were not significantly affected by RT binding. a, DNA-DNA primer-template complexes (black arrows) were labelled with Cy3 (green star) and Cy5 (red star). Both dyes were placed on one end of the 19 nt duplex region. FRET histograms before (red) and after (blue) the addition of 20 μM RT shows quantitatively similar peaks at a high FRET efficiency, indicating that RT did not cause a significant change in the fluorescence properties of the FRET dyes or significant melting of the nucleic-acid substrate. Significant binding to the substrates were already observed at 10 – 20 nM RT (see Figs. 1 and 2 in the main text). **b**, A DNA-DNA substrate with the Cy3 and Cy5 dyes placed on opposite ends of the duplex region. The FRET histograms were similar before and after the addition of 20 μM RT. This is consistent with previous results from crystal structures[20-23], revealing a moderate bending of the duplex substrate induced by RT binding, which only leads to a relatively small change in the end-to-end distance of the DNA duplex.

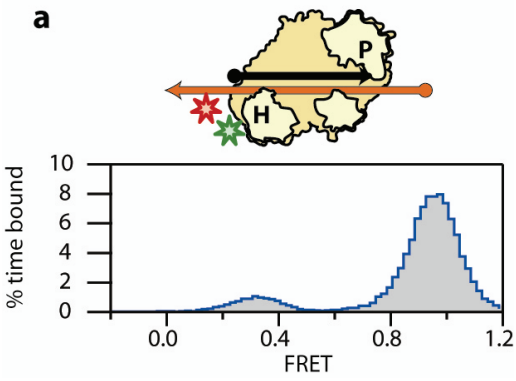

Supplementary Figure 4: Orientation of RT bound to a substrate consisting of a DNA primer and a RNA template. H-labelled RT was allowed to bind to 5*-labelled substrates containing a 19 nt DNA primer annealed to a 50 nt RNA template. RT predominantly bound to the substrate in a high FRET orientation, with the FRET peak position identical to that observed for RT bound to the DNA-DNA primer-template complex.

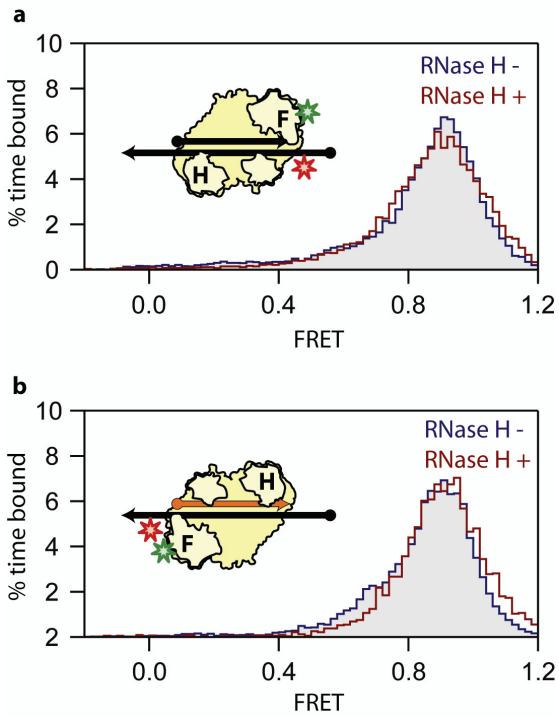

Supplementary Figure 5: Orientation of RNase H active RT bound to DNA-DNA and RNA-DNA primer-template complexes. a, F-labelled RNase H active RT was allowed to bind to 3*-labelled substrates containing a 19 nt DNA primer annealed to a 50 nt DNA template. The presence of the dye label did not abolish the RNase activity of RT. The resulting FRET histogram (red) is nearly identical to that obtained for the RNase inactive (E478Q) mutant bound to the same substrate (blue, identical to Fig. 2c), indicating that the two RT enzymes bound to the DNA-DNA primer-template complex with the same orientation. **b,** F-labelled RNase H active RT was allowed to bind to 5*-labelled substrates containing a 19 nt RNA primer annealed to a 50 nt DNA template. The resulting FRET histogram (red) is again nearly identical to that obtained for the RNase inactive mutant bound to the same substrate (blue, identical to Fig. 2f), indicating that the two RT enzymes also bound to the RNA-DNA primer-template complex with the same orientation. In order to minimize the influence of RNA cleavage by the RNase H active RT, data was only collected for the first 100 seconds after Mg^{2+} was added to the buffer.

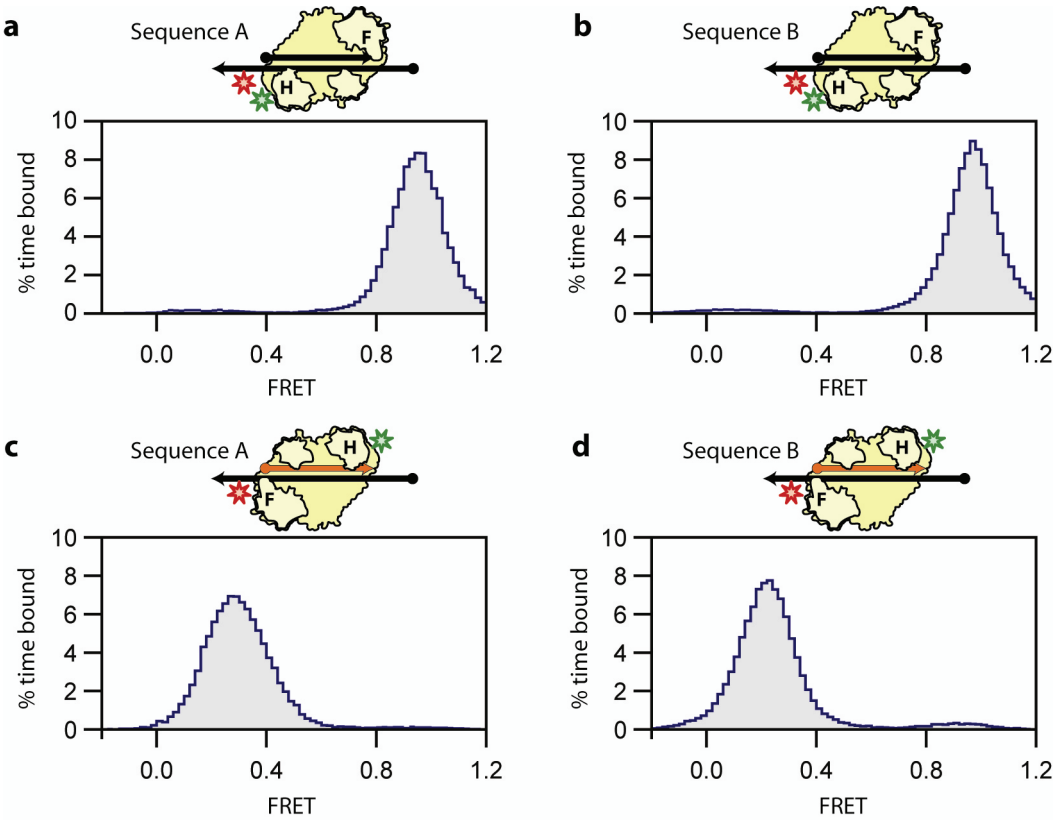

Supplementary Figure 6: Effect of nucleic-acid sequence on the binding orientation of RT. H-labelled RT was allowed to bind to 5*-labelled substrates consisting of DNA templates and DNA (black, upper panels) or RNA (orange, lower panels) primers. In each case, FRET histograms for two different nucleic acid sequences (sequences A and B as shown in Supplementary Fig. 1) were presented for comparison. The sequence A data also appears in Fig. 2, while the Sequence B data also appears in Fig. 3. In each case, RT predominantly adopted a single binding orientation, and the binding configuration was essentially identical for the two different sequences.

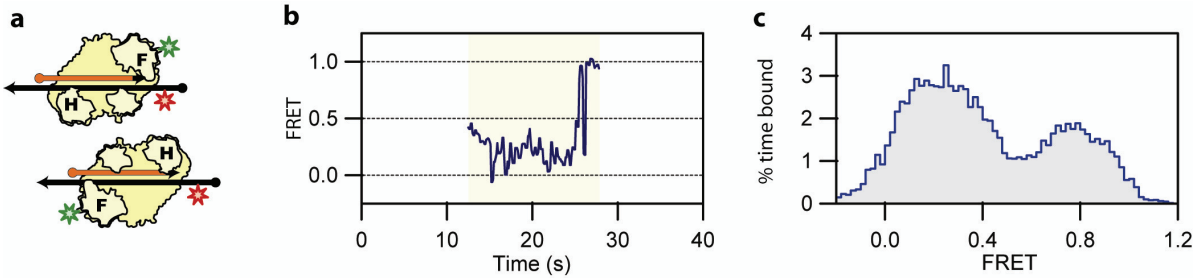

Supplementary Figure 7: Flipping transitions of F-labelled RT on a 3*-labelled substrate. **a**, To further support the observation that RT flips between opposite binding orientations, we measured the orientational dynamics of RT bound to the PPT:d2 substrate using an alternative pair of labelling sites. In contrast to Fig. 5, where H-labelled RT was allowed to bind 5*-labelled substrates, here F-labelled RT was allowed to bind 3*-labelled PPT:d2 substrates (PPT RNA in orange and 2 nt of DNA extension in black) annealed to DNA templates. **b**, FRET trajectory of a single binding event showing multiple flipping transitions. **c**, FRET histogram constructed from multiple binding events. The F-labelled RT produces broader FRET peaks than H-labelled RT (compare to Fig. 5c) but the ratio between the residence times that RT spent in the two orientation was nearly identical (2.2 for F-labelled RT on 3*-labelled substrate vs. 2.3 for H-labelled RT on 5*-labelled substrate). A broader peak was also observed when F-labelled RT was bound to pure RNA or DNA primers (Figs. 2c, f), potentially reflecting conformational dynamics within the polymerase fingers and thumb sub-domains of RT.

a

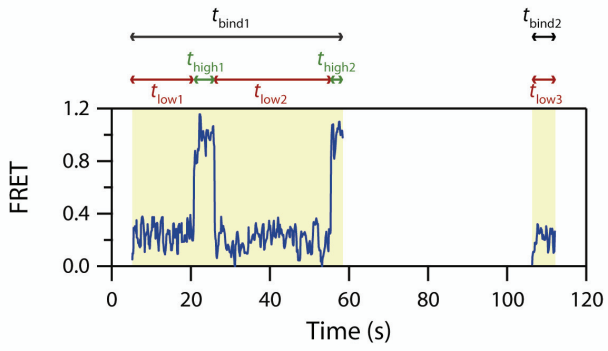

b

	τ_{low}	τ_{high}	τ_{bind}	N_{low}	N_{high}	N_{bind}
PPT	18±2 s	5.6±1.3 s	17±2 s	189	220	282
PPT:d2	13±1 s	3.8±0.5 s	13±1 s	258	398	397
PPT:dd2	13±1s	5.0±0.3 s	11±1 s	368	790	828
PPT:dd2+dTTP	18±4 s	52±4 s	52±4 s	85	245	280
PPT:d2+Nevirapine	11±0.9 s	2.3 ±0.3 s	34±3 s	516	485	341

c

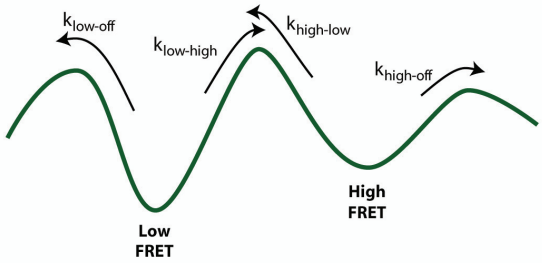

d

	$k_{low-off}$	$k_{low-high}$	$k_{high-low}$	$k_{high-off}$
PPT	2.3±0.4 min^{-1}	1.2±0.3 min^{-1}	3.1±1.9 min^{-1}	7.6±4.5 min^{-1}
PPT:d2	2.3±0.4 min^{-1}	2.3±0.4 min^{-1}	5.2±1.0 min^{-1}	11±2 min^{-1}
PPT:dd2	2.5±0.4 min^{-1}	2.0±0.4 min^{-1}	2.5±0.4 min^{-1}	9.5±0.6 min^{-1}
PPT:dd2+dTTP	2.4±1.2 min^{-1}	1.0±0.7 min^{-1}	0.12±0.06 min^{-1}	1.0±0.1 min^{-1}
PPT:d2+Nevirapine	1.9±0.3 min^{-1}	3.4±0.3 min^{-1}	18±3 min^{-1}	8.3±1.7 min^{-1}

Supplementary Figure 8: Kinetic analysis of the flipping transitions of RT. a, An example FRET trace showing RT binding to a single substrate. Two binding events were observed in this trace, and the duration of each was measured. The FRET value within each binding event can be further divided into low and high FRET sub-states. The duration of each sub-state was also determined. **b**, The table lists the following data derived from many binding events on various substrates: The mean residence time spent in the low FRET sub-state (τ_{low}), the mean residence time spent in the high FRET sub-state (τ_{high}), the mean time RT was bound to the substrate

(τ_{bind}), the total number of low FRET events measured (N_{low}), the total number of high FRET events measured (N_{high}), and the total number of binding events collected (N_{bind}). **c**, A simple kinetic model of flipping and dissociation, featuring four first-order rate constants. $k_{low\text{-}off}$: dissociation rate constant from the low FRET orientation, $k_{low\text{-}high}$: flipping rate constant from the low FRET to the high FRET orientation, $k_{high\text{-}low}$: flipping rate constant from the high FRET to the low FRET orientation, and $k_{high\text{-}off}$: dissociation rate constant from the high FRET orientation. **d**, The table lists the kinetic rate constants derived from the measure parameters given in (b) using the kinetic model shown in (c). The formulas used to calculate the data were as follows, assuming the system was at equilibrium:

- $k_{low\text{-}off} = (1/\tau_{low})\cdot P_{low\text{-}off} = (1/\tau_{low})\cdot(N_{bind}+N_{low}-N_{high})/(2\cdot N_{low})$
- $k_{low\text{-}high} = (1/\tau_{low})\cdot P_{low\text{-}high} = (1/\tau_{low})\cdot(N_{high}+N_{low}-N_{bind})/(2\cdot N_{low})$
- $k_{high\text{-}low} = (1/\tau_{high})\cdot P_{high\text{-}low} = (1/\tau_{high})\cdot(N_{high}+N_{low}-N_{bind})/(2\cdot N_{high})$
- $k_{high\text{-}off} = (1/\tau_{high})\cdot P_{high\text{-}off} = (1/\tau_{high})\cdot(N_{bind}+N_{high}-N_{low})/(2\cdot N_{high})$

where $P_{low\text{-}off}$ is the probability of dissociation once RT is bound in the low FRET state, $P_{low\text{-}high}$ is the probability of flipping to the high FRET state once RT is bound in the low FRET state, $P_{high\text{-}low}$ is the probability of flipping to the low FRET state once RT is bound in the high FRET state, and $P_{high\text{-}off}$ is the probability of dissociation once RT is bound in the high FRET state. The system was assumed to be at equilibrium. All errors were estimated using the bootstrap technique[42]. As shown by these data, all rate constants are similar for the PPT, PPT:d2 and PPT:dd2 substrates in the absence of small molecule additives. The rate constants of leaving the low FRET state, including both the dissociation rate constant from the low FRET state ($k_{low\text{-}off}$) and the flipping rate constant from the low FRET to the high FRET orientation ($k_{low\text{-}high}$) did not vary significantly upon addition of either the cognate nucleotide dTTP or the NNRTI Nevirapine, whereas the rate constants of leaving the high FRET state were significantly more sensitive these small molecules. In the presence of dTTP, both the dissociation rate constant from the high FRET state ($k_{high\text{-}off}$) and the flipping rate constant from the high FRET to the low FRET orientation ($k_{high\text{-}low}$) decreased drastically (compare the PPT:dd2 + dTTP and PPT:dd2 cases in d). In contrast, the addition of Nevirapine substantially increased $k_{high\text{-}low}$ without significantly affecting $k_{high\text{-}off}$ (compare the PPT:d2 + Nevirapine and PPT:d2 cases in d).

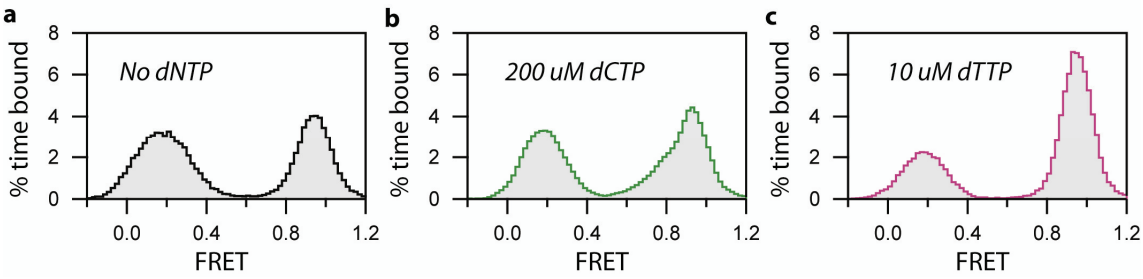

Supplementary Figure 9: Effect of non-cognate vs. cognate dNTP on the binding orientation of RT. FRET histogram of H-labelled RT binding to the 5*-labelled PPT:dd2 substrate in the absence of nucleotides (**a**), in the presence of 200 μM dCTP (**b**) and in the presence of 10 μM dTTP (**c**). Whereas dCTP was not complimentary to next position on the template strand and had little effect on the orientational distribution of RT, the cognate nucleotide dTTP caused a significant shift towards the high FRET state even at a lower concentration.

References:

42. Efron, B. & Gong, G. A Leisurely look at the bootstrap, the Jackknife, and cross-validation. *Amer. Statistician* **37**, 36-48 (1983)